Prediction of Dissolution Behaviour of Fumaric Acid (Form A) Using Molecular Modelling

Nur Azmina Mohd Rabi, Siti Nurul'ain Yusop, Nornizar Anuar, Muhammad Fitri Othman

Faculty of Chemical Engineering, Universiti Teknologi Mara

***Abstract*— In this study, a dissolution prediction of fumaric acid (Form A) in ethanol solvent was investigated using molecular dynamic simulation. Five important facets were selected for this study which are (0 2 0), (1 0 0), (0 1 1), (-1 1 0) and (1 1 -1). The dissolution prediction of fumaric acid (Form A) was analysed using radial distribution function (RDF) for molecular interactions analysis and mean square displacement (MSD) for diffusion coefficient values, D. Based on the analysis, facet (0 1 1) is the fastest facet to dissolve in ethanol and (1 0 0) facet is the last facet to dissolve in solvent. The correlation between radial distribution function and mean square displacement is the lower peak for RDF indicated the distance of fumaric acid for unrigid atom is closed with reference atom which exist with hydrogen bond. The MSD is proved that hydrogen bond is more difficult to break and display lower diffusion coefficient, D in the system.**

Keywords*— Dissolution, fumaric acid, mean square displacement, radial distribution function, diffusion coefficient

I. Introduction

The Fumaric acid or in synthetic name called trans-butenedioic acid is an intermediate in the tricarboxylic acid cycle for organic acid biosynthesis. It is the most important agents in food industry (Dallos, Hajós-Szikszay, & Liszi, 1998). The crucial step in drug absorption from solute which oral solid dosage forms is dissolve in a solvent called dissolution. It occurs when a process of drug molecules disintegrated from the solid particle and into the surrounding gastrointestinal (GI) milieu (Gao & Olsen, 2013). Mostly, drug is more soluble in empty stomach which contain low pH. However, drug usually take after meals to avoid gastric content where the pH is increase when consume the food and solubility of drug also decreases (Nadendla, 2008). Crystal engineering methods development like co-crystallisation functions to controlled crystallisation of drugs or active site of drugs to create high purity with referred the crystal habit, surface of nature, surface energy, particle size distribution and also crystal form either in crystalline and amorphous form. Usage of different solvents, rate of stirring of combination with other component like salts can be change or produce packaging arrangement which called polymorphs (Savjani, Gajjar, & Savjani, 2012). The advantages using co-crystal method is can be stabilized crystalline form such as amorphous solids which no need to change or destroy covalent bond of atomic atom itself. Therefore, co-crystal technique also capable use in both types of API molecules to form co-crystal either have weakly ionisable or non-ionisable (Yadav, Shete, Dabke, Kulkarni, & Sakhare, 2009). Fumaric acid as a co-former has been success combine with an active pharmaceutical ingredient (API) such as carbamazepine (Rahman, Rahim, Chou, Low, & Ramle, 2017), fluoxetine hydrochloride (Scott L. Childs et al., 2004) and nilotinib hydrochloride (Viertelhaus & Hafner, 2015). Function of co-former is to help the active pharmaceutical ingredient (APIs) or can be called as drug to disintegrate into small particles to be transported to the blood stream but still protect the stability of product so it will be at greatest benefits (Rahman et al., 2017). Co-crystal formation methods usually faced a challenging situation where the preparation of co-crystal has been known to take 6 months to prepare a single co-crystal of suitable quantity or stoichiometry for single X-ray diffraction (XRD) analysis that describe in the literature (Yadav et al., 2009). There are two techniques to prepare co-crystal which are traditional method and novel method. For traditional method include solution method, solvent evaporation, slurry conversion and grinding method while novel method includes heat-introduced, co-crystallisation, spray drying, supercritical fluid (SCF) technology and also laser irradiation (Zu'aimah Barikah, 2018). Some APIs cannot be used as drug applicants because they have got poor solubility and inefficient bioavailability. Hence, co-crystallization approach is the strategy for them improving their solubility and bioavailability without changing the inherent bioactivity of the APIs of interest by predict the correct physical properties or dissolution behaviour using molecular modelling.

Molecular modelling refers for the general process of describing complex chemical systems with the aim of understanding and predicting macroscopic properties based totally on specific data at an atomic scale. In this study, molecular modelling is used to predict the correct physical properties or dissolution behaviour and molecular interactions of fumaric acid and ethanol using mean square displacement (MSD) and radial distribution function (RDF). MSD is function to determine the particle position versus time (ps) by mean the particle is dispersed cause of diffusion through the environment which is the bulk solvent. The MSD of the particles with respect to the original position or reference is related to the diffusion coefficient (D). Meanwhile, RDF evaluated the atoms are actually radially packed with each other in a solution which are with hydrogen bonds or composed with Coulomb and Van der Waals forces.

Hydrogen bond interaction is become the important character for formation of crystal structure (Hayakawa, Ueda, Yamane, Miyamoto, & Horii, 2011). Hydrogen bond always occurs in between proton donor which is hydrogen atom and attached with the most electronegative like -OH group, nitrogen, fluoride and oxygen and a proton acceptor (O), have two lone airs of electrons

(Mosapour Kotena, Behjatmanesh-Ardakani, Hashim, & Manickam Achari, 2013), (Nornizar Anuar et al., n.d.). MD simulation is conducted in room temperature because hydrogen bond can form easily at the lower temperature.

II. METHODOLOGY

A. Crystal Structure

The structure of fumaric acid (Form A) file ref. code: FUMAAC) was extracted from the Cambridge Structural Database (CSD). Form A polymorph crystallised in monoclinic cell system with $P2_1/c$ space group and cell parameters of a = 7.619 Å, b = 15.014 Å, c = 6.686 Å, α= 90°, β = 112°, γ= 90°(Brown, 1996). It comprises 14 molecules in a unit cell of crystal. Figure 1 shows the molecular structure of fumaric acid (Form A) in x-, y- and z-directions.

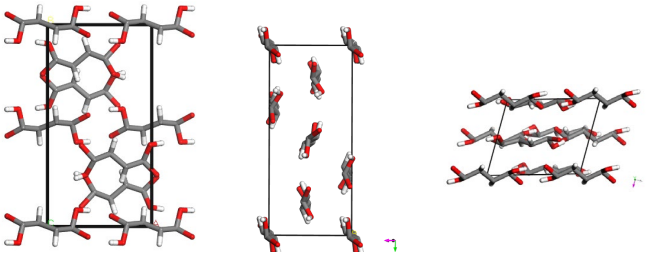

(a) (b) (c)

Figure 1: Molecular structure of fumaric acid (Form A) crystal lattice in (a) x-direction, (b) y-direction and (c) z-direction (Nurul, Nili, Anuar, Azmi, & Othman, 2018)

B. Molecular Modelling Method

Molecular modelling simulation was conducted to predict the dissolution behaviour of fumaric acid (Form A) in ethanol (solvent) by using Material Studio software version 7.0 from Accelrys. The analysis of the mean square displacement (MSD) and radial distribution function (RDF) was carried out to assess the diffusion rate and bonding interactions within crystal, respectively. The predicted morphology of fumaric acid (Form A) shows in Figure 2 was cleaved with 2.0 thickness layer and enlarge to 3D periodic supercell for every facet chosen for dynamic simulation. Five facets were chosen which are (020), (011), (100), (-110) and (11-1) based on the morphological important facets and attachment energy values. Table 1 shows different value for U, V directions and thickness of vacuum slab for every facet.

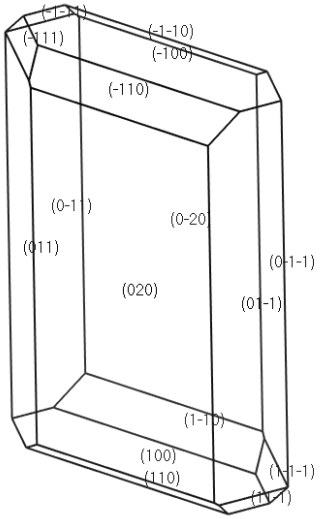

Figure 2: The predicted morphology of fumaric acid (Form A) (Nurul et al., 2018)

Table 1: Value of U, V direction and vacuum slab thickness

Facet	U direction	V direction	Vacuum slab thickness (Å)
(020)	6	5	25
(011)	4	2	20
(100)	3	7	25
(-110)	5	2	17
(11-1)	3	5	30

C. Construction of 3D Periodic Structure of Ethanol

One molecule of ethanol was created in a periodic amorphous cell module at 298 K. Then the molecule was inserted into the vacuum slab above the cleaved surface of fumaric acid form A. The position of ethanol molecule should be placed on the cleaved surface with the existence of hydrogen bonding between ethanol and fumaric acid molecule.

D. Geometry optimization

All crystal surface was kept constraint for geometry optimization except ethanol solvent. The crystal was optimised using Dreiding forcefield and CVFF forcefield were used from the previous charge calculation when build morphology of the fumaric acid (Form A) crystal.

E. Dynamic Simulation for Dissolution of Fumaric Acid (Form A)

Dynamic simulation was run using CVFF forcefield. In this step, forcefield assigned charge was used because the value of total energy is more stable compared to the other charges. Before the simulation, the upper layer of crystal was set to be unconstrained and the lower layer kept constraint. The dynamic simulation was using constant NVT (number of molecules, volume and temperature) at 25°C and the temperature was controlled using Nosé-Hoover thermostat. Total simulation time is 1 ns (1000 ps) with 1 fs time step and the frame output was recorded for every 2000 steps.

F. Analytical Descriptions of MD Simulation Results

1) Radial distribution function (RDF)

The radial distribution function (RDF) encourage to analyses the binding process and assisted by ethanol (Sneha & Priya Doss, 2016) and evaluated how the atoms are radially packed around each other in a solution within observe the specific interactions especially hydrogen bonding and Coulomb and Van der Waals forces.

2) Mean square displacement

Mean square displacement also an analytical method to confirm the analysis. Mean square displacement is determined the displacement of selected molecules in one-unit cell from its original position versus time (ps) by mean the particle is diffuse cause of diffusion through the environment which is the solvent. The slope of MSD is used to calculate the diffusion coefficients, D by the Einstein relation equation below (Concu & Cordeiro, 2016).

$$D = \frac{1}{6}\lim_{t\to\infty}\frac{d}{dt}\sum_{i=1}^{N_a}\langle|r_i(t) - r_i(0)|^2\rangle \quad (1)$$

where r_i means the position vector of an i_{th} particle and the angular brackets means an ensemble average. D is measured by the slope of the MSD versus time in ps. After the equation (1) is modified, the new equation, Eq. (2) is used.

$$MSD = \langle |\bar{r} - \overline{r^0}|^2 \rangle = 2nDt \quad (2)$$

MSD will be calculated based on MD simulation that performed in 3D, therefore, n = 3. Then, the equation can be simplified into Eq. (3) (Wang & Hou, 2011):

$$D = \frac{slope}{6} \quad (3)$$

III. RESULTS AND DISCUSSION

A. Dissolution Behavior of Fumaric acid (Form A) in Ethanol

Molecular dynamic (MD) simulation was run to assess the molecular interactions and diffusion behaviour of crystal molecules at the surface and solvent. Figure 3 shows the cleaved facets with one ethanol molecule in vacuum slab that positioned based on the existence of hydrogen bonding interactions between crystal molecule and ethanol molecule. Selection of one unit cell of crystal molecule and reference molecule is based on the position of ethanol towards crystal molecules after geometry optimisation. Difference colours were used to differentiate the selected crystal molecules in one unit cell and the reference molecule.

(i) Before dynamic simulation

a. (0 2 0)

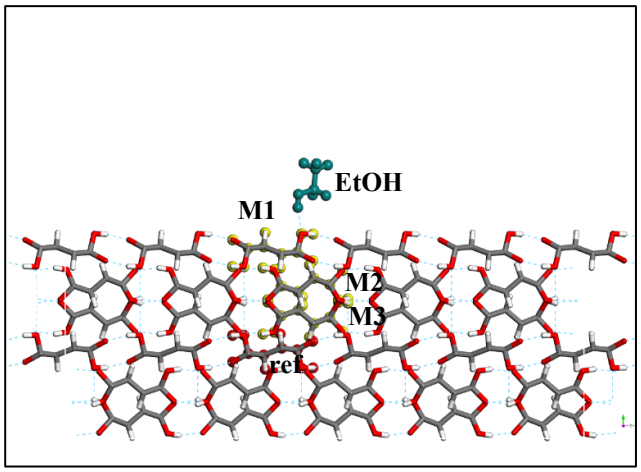

b. (1 0 0)

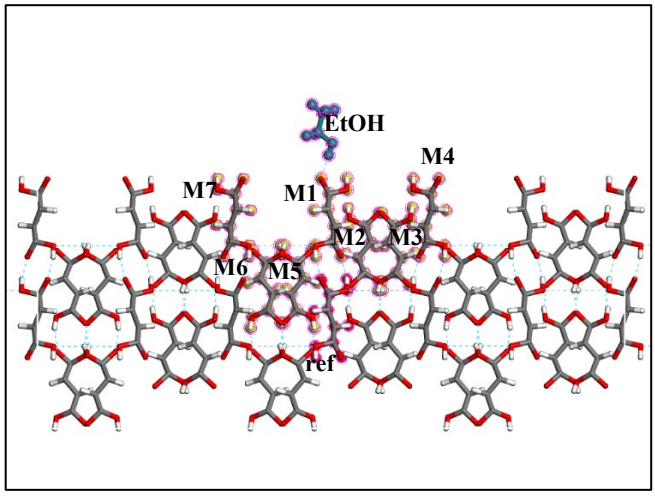

c. (0 1 1)

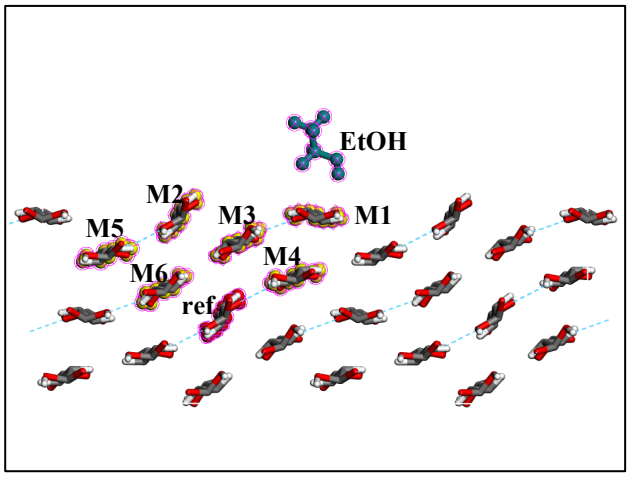

d. (-1 1 0)

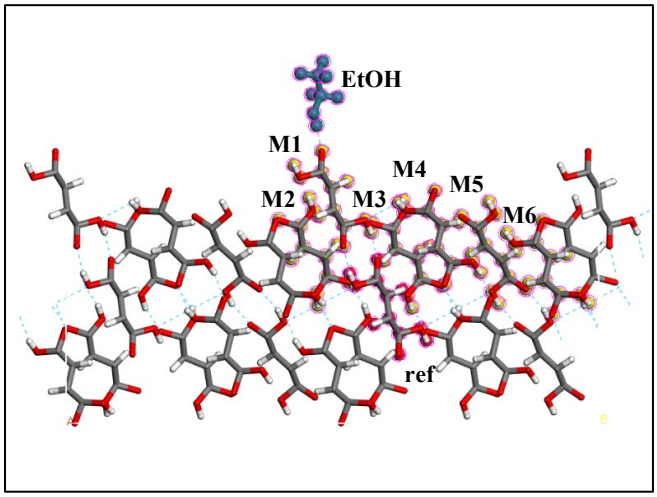

e. (1 1 -1)

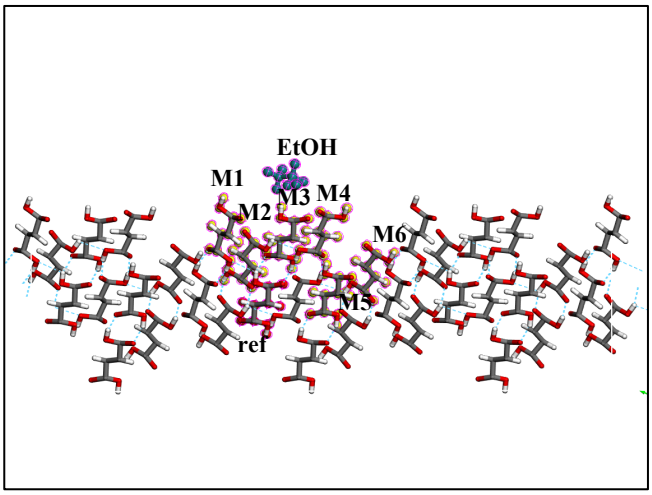

(ii) After dynamic simulation

a) (0 2 0)

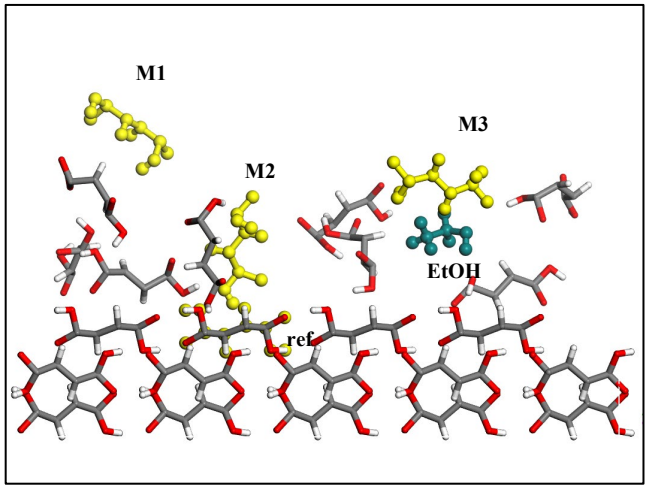

b) (1 0 0)

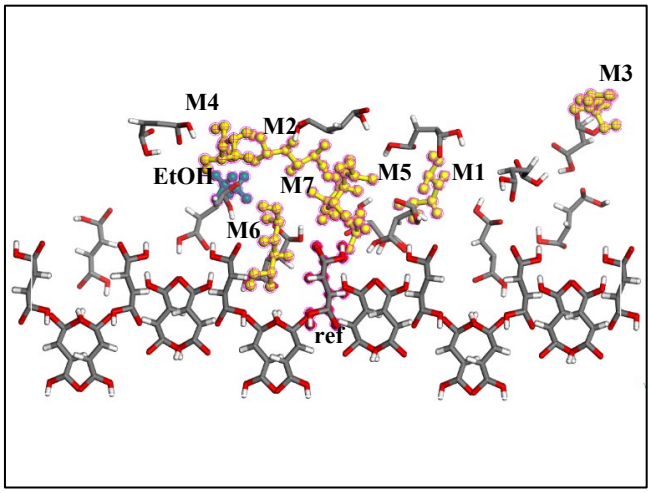

c) (0 1 1)

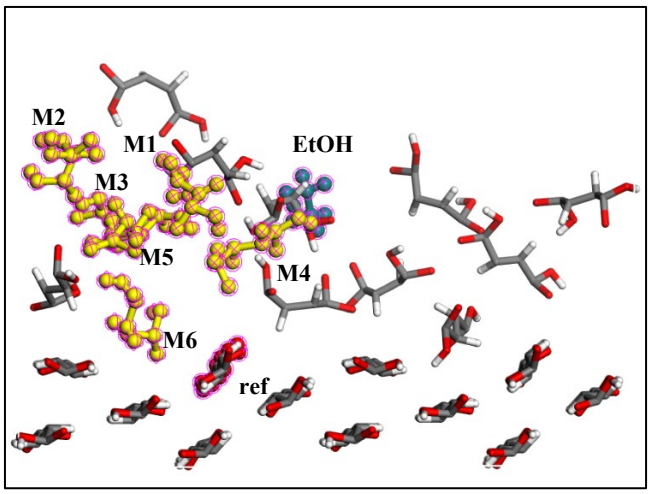

d) (-1 1 0)

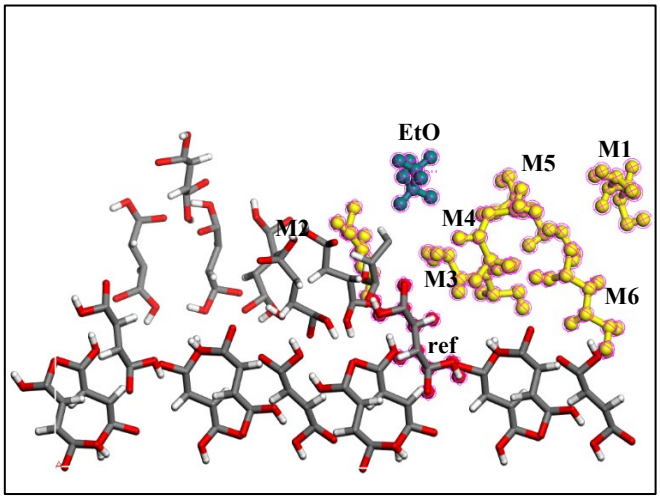

e) (1 1 -1)

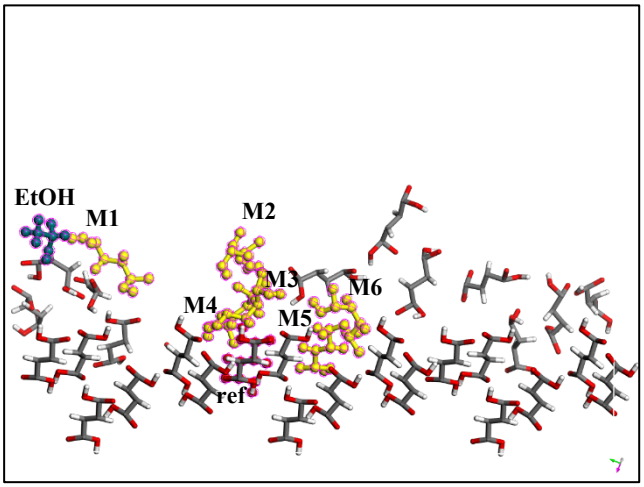

Figure 3: The position of ethanol molecule on the surface of (a) (0 2 0), (b) (1 0 0), (c) (0 1 1), (d) (-1 1 0) and (e) (1 1 -1) in vacuum slab (i) before and (ii) after dynamic simulation

B. Radial distribution function (RDF)

Figure 4 shows the peaks of the RDF results for selected molecules for every facet while Table 2 tabulates the values of the earliest peaks came out from RDF analysis for the selected molecules.

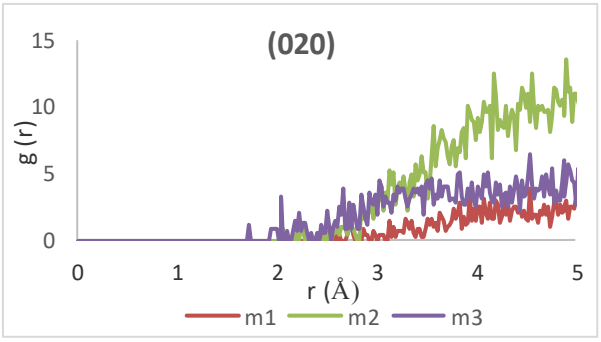

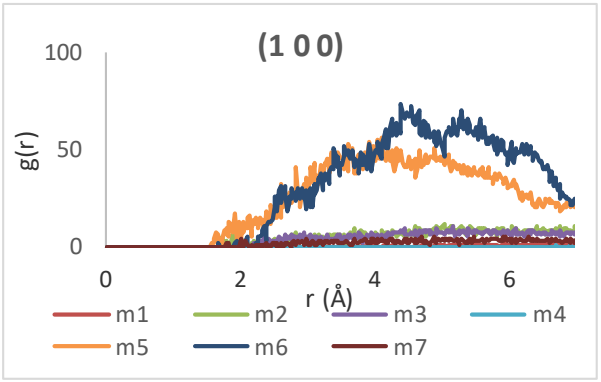

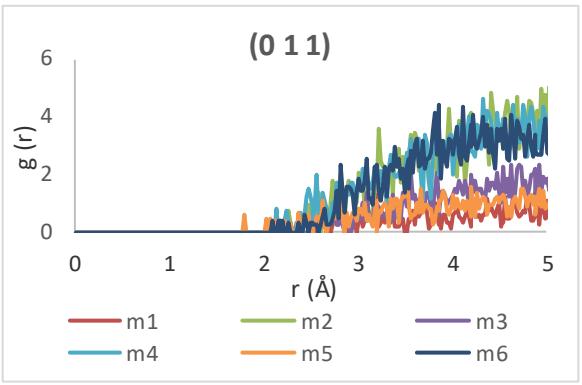

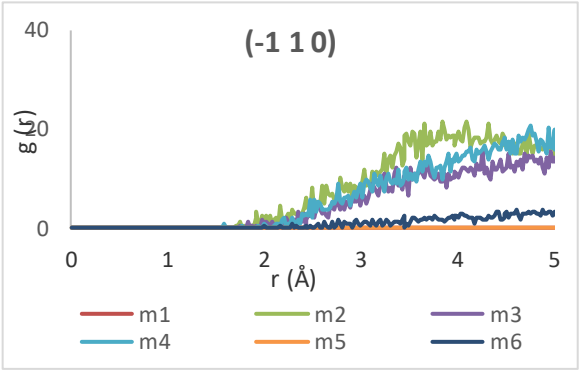

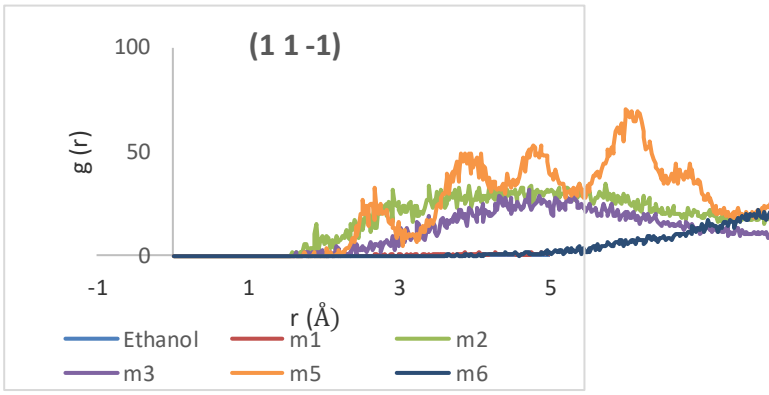

Figure 4: RDF graph of facet (0 2 0), (1 0 0), (0 1 1), (-1 1 0) and (1 1 -1)

Table 2: First peak value of RDF peak for each molecule to reference molecule for every facet

Facet	(0 2 0)	(1 0 0)	(0 1 1)	(-1 1 0)	(1 1 -1)
M1	2.21	1.91	2.37	3.27	2.35
M2	2.07	1.73	2.27	1.71	1.59
M3	1.71	2.01	2.51	1.75	1.63
M4	-	6.73	2.13	1.59	1.61
M5	-	1.59	1.79	4.39	1.75
M6	-	1.69	2.09	2.01	3.63
M7	-	1.79	-	-	-

Fumaric acid (Form A) shows different peaks equivalent to the separation between the crystal lattice. The magnitude of peaks, g(r) related with the number of particles that close to that atom (Shi, Chu, Xia, Lei, & Wang, 2016). In radial distribution graph, the first peak were observed and if the peak appears within the range of 0 to 0.35 nm, it means the interactions contributed by hydrogen bonds. If the first peak is higher than 3.5 Å the interactions mainly contributed by Coulomb and Van der Waals forces (Shi, Xia, Lei, & Wang, 2014). For (0 2 0) facet, there are three molecules was selected for the analysis. The first peak values for all three molecules are below 3.5 Å which are 2.21, 2.07 and 1.71 for M1, M2, and M3, respectively. It can be seen from Figure 3 that M3 has the shortest distance between M3 molecule to the reference molecule. Therefore, the hydrogen bonding interaction is stronger compared to the other 2 molecules. The stronger hydrogen bonding depend on the shorter distance of hydrogen bond between atom (Nornizar Anuar et al., n.d.). The contribution of hydrogen bonding interactions can be observed from the RDF result between selected molecules in the unit cell for five facets to the reference molecule except for M4 molecule at (1 0 0) facet that has greater than 3.5 Å. It means only van der Waals interactions exist between M4 molecule and the reference molecule. It can be seen from Figure 4 (b (ii)) (after dynamic simulation) that the position of M4 molecule far from the reference molecule. It is because the position of M4 itself was far from the reference molecule, hence, no hydrogen bonding exists.

C. Mean Square Displacement (MSD)

MSD graph for every facet for fumaric acid (Form A) are presented in Figure 5. The slope of MSD illustrated the displacement of the molecule from its original position and the movement molecule in the system as shown in Table 4.

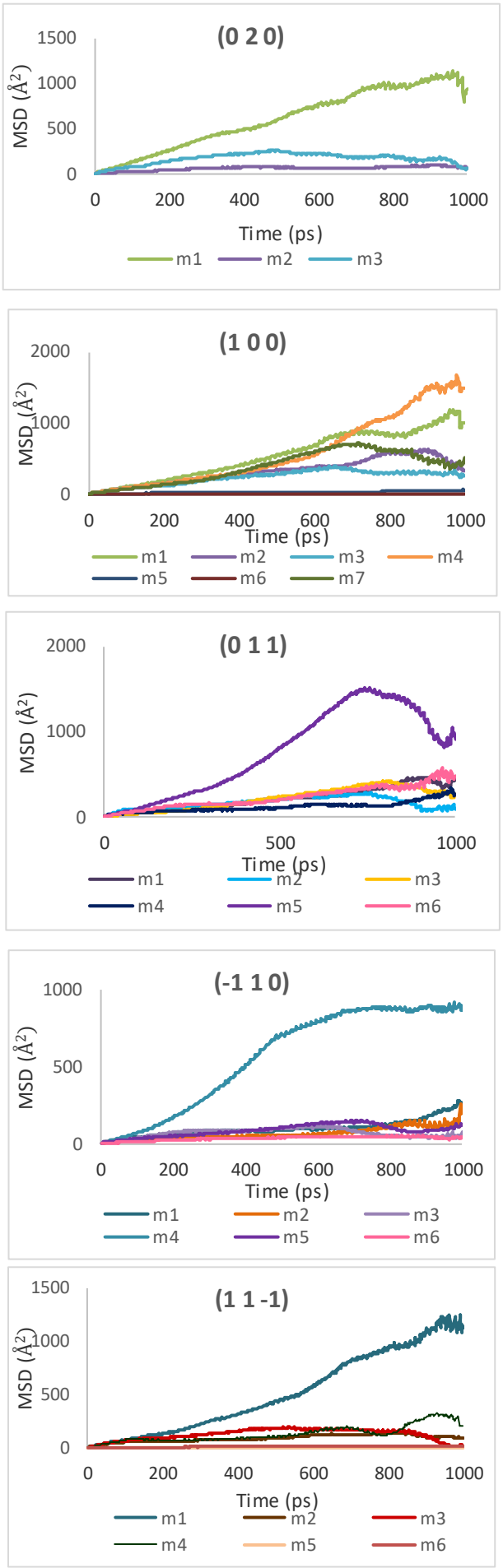

Figure 5: MSD graph of fumaric acid (Form A)

Table 4: The value of diffusion coefficient (D) for facet fumaric acid (Form A), (m^2/s)

Facet	(0 2 0)	(1 0 0)	(0 1 1)	(-1 1 0)	(1 1 -1)
M1	2E-09	1.92E-09	5.26E-10	2.77E-10	1.44E-09
M2	8.43E-10	1.01E-09	5.2E-10	1.48E-10	1.42E-10
M3	2.66E-10	8.97E-10	5.27E-10	2.99E-10	4.99E-10
M4	-	1.5E-09	3.58E-10	2.25E-09	8.15E-11
M5	-	4.3E-11	1.89E-09	2.96E-10	1.17E-12
M6	-	2E-12	9.15E-10	1.33E-10	2.65E-11
M7	-	1.69E-09	-	-	-

For (0 2 0) facet, M1 molecule has the highest diffusion coefficient, $2.0x10^{-9}$ m^2/s. This can be seen in Figure 4 that the position of M1 molecule is far from the reference molecule. This can be supported by RDF result that shows the RDF value for M1 molecule is higher compared to M2 and M3 molecule in which the position of both molecules are closer to the reference molecule. For (1 0 0) facet, M1 molecule has the highest diffusion coefficient value whilst M6 molecule is the lowest value. (1 1 -1) facet, the highest diffusion coefficient is M1 while for (0 1 1) is M5 and (-1 1 0) is M4. It can be seen that the highest diffusion coefficient has a steep slope compared to the other molecule. The molecules that have lowest diffusion coefficients for (0 2 0), (1 0 0), (0 1 1), (-1 1 0) and (1 1 -1) are M2, M6, M6, M3 and M5, respectively. The high diffusion coefficients presented the molecule have weak hydrogen bonding interactions of selected molecules to the reference molecule. Therefore, the molecules can detach easily from the rigid crystal and diffuse from crystal to the environment. The MSD graph and calculated diffusion coefficient values supported by the result of dynamic simulation with different frame in Figure 4. The further of molecules dispersed from its original position describe the stronger movement of molecules in the system. Nonetheless, molecules have low mobility in the cell due to several disturbances that make them retrain the movement such as the molecule have strong hydrogen bond with rigid molecule (reference) or unrigid crystal around them (N. Anuar et al., 2018). However, the molecule that near to the solvent molecule will easily diffuse to the environment. For example, facet (0 2 0) the hydrogen bond exists between molecule M1 and reference molecule more easily diffuse to environment compared to M3 in which has stronger hydrogen bonding towards the reference molecule.

CONCLUSION

The correlation between radial distribution function and mean square displacement is the lower peak for RDF indicated the distance of fumaric acid for unrigid atom is closed with reference atom include with hydrogen bond. The MSD is proved that hydrogen bond is more difficult to break and display lower diffusion coefficient, D in the system.

ACKNOWLEDGMENT

Thank you to my supervisor Dr. Siti Nurul 'Ain Yusop, other lecturer Dr. Nornizar Anuar, En. Muhammad Fitri Othman and Faculty of Chemical Engineering, Universiti Teknologi Mara Shah Alam for providing research facilities to complete this work.

References

Anuar, N., Pauzi, N. S., Ain Yusop, S. N., Azmi, N. S. M., Rahim, S. A., & Othman, M. F. (2018). Prediction of carbamazepine-succinic acid co-crystal dissolution in ethanolic solution using a computational

molecular dynamic simulation technique. *International Journal of Engineering and Technology(UAE)*, *7*(4), 122–128.

Anuar, Nornizar, Nor, W. A. N., Wan, A., Daid, M., Khalid, S. A., Fauziah, S., … Abdullah, R. S. (n.d.). *Prediction of Interaction of Citric Acid Modified Cellulose with Water Region Using Molecular Modelling Technique*.

Brown, C. J. (1996). The crystal structure of fumaric acid. *Acta Crystallographica*, *21*(1), 1–5. https://doi.org/10.1107/s0365110x66002226

Concu, R., & Cordeiro, M. N. D. S. (2016). Molecular dynamics simulation study of the selectivity of a silica polymer for ibuprofen. *International Journal of Molecular Sciences*, *17*(7), 1–11. https://doi.org/10.3390/ijms17071083

Dallos, A., Hajós-Szikszay, É., & Liszi, J. (1998). Enthalpies of solution and crystallization of L-ascorbic acid in aqueous solution. *Journal of Chemical Thermodynamics*, *30*(2), 263–270. https://doi.org/10.1006/jcht.1997.0298

Gao, Y., & Olsen, K. W. (2013). Molecular dynamics of drug crystal dissolution: Simulation of acetaminophen form I in water. *Molecular Pharmaceutics*, *10*(3), 905–917. https://doi.org/10.1021/mp4000212

Hayakawa, D., Ueda, K., Yamane, C., Miyamoto, H., & Horii, F. (2011). Molecular dynamics simulation of the dissolution process of a cellulose triacetate-II nano-sized crystal in DMSO. *Carbohydrate Research*, *346*(18), 2940–2947. https://doi.org/10.1016/j.carres.2011.10.019

Mosapour Kotena, Z., Behjatmanesh-Ardakani, R., Hashim, R., & Manickam Achari, V. (2013). Hydrogen bonds in galactopyranoside and glucopyranoside: A density functional theory study. *Journal of Molecular Modeling*, *19*(2), 589–599. https://doi.org/10.1007/s00894-012-1576-z

Nadendla, R. R. (2008). Molecular modeling: A powerful tool for drug design and molecular docking. *Resonance*, *9*(5), 51–60. https://doi.org/10.1007/bf02834015

Nurul, S., Nili, W. A., Anuar, N., Azmi, N. S., & Othman, M. F. (2018). Dissolution Prediction of Fumaric Acid Crystal (Form A) in Ethanol using Molecular Dynamic Simulation. *International Journal of Engineering and Technology*, *7*(4.18), 483–487.

Rahman, F. A., Rahim, S. A., Chou, C. T., Low, S. H., & Ramle, N. A. (2017). Carbamazepine-Fumaric Acid and Carbamazepine-Succinic Acid Co-crystal Screening Using Solution Based Method. *International Journal of Chemical Engineering and Applications*, *8*(2), 136–140. https://doi.org/10.18178/ijcea.2017.8.2.645

Savjani, K. T., Gajjar, A. K., & Savjani, J. K. (2012). Drug Solubility: Importance and Enhancement Techniques. *ISRN Pharmaceutics*, *2012*(100 mL), 1–10. https://doi.org/10.5402/2012/195727

Scott L. Childs, *, Leonard J. Chyall, ‡, Jeanette T. Dunlap, ‡, Valeriya N. Smolenskaya, ‡, Barbara C. Stahly, ‡ and, & Stahly‡, G. P. (2004). Crystal Engineering Approach To Forming Cocrystals of Amine Hydrochlorides with Organic Acids. Molecular Complexes of Fluoxetine Hydrochloride with Benzoic, Succinic, and Fumaric Acids. *Journal of the American Chemical Society*, (2), 13335–13342. https://doi.org/10.1021/JA048114O

Shi, W., Chu, Y., Xia, M., Lei, W., & Wang, F. (2016). Crystal morphology prediction of 1,3,3-trinitroazetidine in ethanol solvent by molecular dynamics simulation. *Journal of Molecular Graphics and Modelling*, *64*, 94–100. https://doi.org/10.1016/j.jmgm.2016.01.004

Shi, W., Xia, M., Lei, W., & Wang, F. (2014). Solvent effect on the crystal morphology of 2,6-diamino-3,5- dinitropyridine-1-oxide: A molecular dynamics simulation study. *Journal of Molecular Graphics and Modelling*, *50*, 71–77. https://doi.org/10.1016/j.jmgm.2014.03.005

Sneha, P., & Priya Doss, C. G. (2016). Molecular Dynamics: New Frontier in Personalized Medicine. In *Advances in Protein Chemistry and Structural Biology* (1st ed., Vol. 102). https://doi.org/10.1016/bs.apcsb.2015.09.004

Viertelhaus, M., & Hafner, A. (2015). Co-crystals and their advantages for APIs with challenging properties. *Chimica Oggi - Chemistry Today*, *33*(5), 23–26.

Wang, J., & Hou, T. (2011). Application of molecular dynamics simulations in molecular property prediction II: Diffusion coefficient. *Journal of Computational Chemistry*, *32*(16), 3505–3519. https://doi.org/10.1002/jcc.21939

Yadav, A., Shete, A., Dabke, A., Kulkarni, P., & Sakhare, S. (2009). Co-crystals: A novel approach to modify physicochemical properties of active pharmaceutical ingredients. *Indian Journal of Pharmaceutical Sciences*, *71*(4), 359. https://doi.org/10.4103/0250-474x.57283

Zu'aimah Barikah, K. (2018). Traditional and novel methods for cocrystal formation: A mini review. *Systematic Reviews in Pharmacy*, *9*(1), 79–82. https://doi.org/10.5530/srp.2018.1.15